Systematics of the (^{3}He,p) reaction on some f-shell nuclei*

Gerald Hardie
Western Michigan University, Kalamazoo, Michigan 49001
and Argonne National Laboratory, Argonne, Illinois 60439

David Gloeckner, L. Meyer-Schützmeister, and T. H. Braid
Argonne National Laboratory, Argonne, Illinois 60439

(Received 19 August 1974)

Using the Argonne split-pole magnetic spectrograph, the ^{43}Ca(^{3}He,p)^{45}Sc reaction was studied at $E(^3\text{He}) = 17$ MeV and with a range of angles from 7 to 55°. From the measured proton angular distributions the orbital angular momenta transferred (L_{np}) by the n-p pair were obtained. In addition, at the same bombarding energy and at several angles, cross sections for $L_{np} = 0$ and $0+2$ were measured for the (^{3}He,p) reaction with ^{46,48,50}Ti and ^{45}Sc targets. For these and other f-shell nuclei, systematics of the cross sections for $L_{np} = 0$ and the sum of the differential cross sections for $L_{np} = 0+2$ will be discussed. In particular we found that for odd-A targets the $L_{np} = 0+2$ sums are significantly smaller than the average for even-even f-shell targets. Two-particle spectroscopic amplitudes are calculated for transitions to ^{44}Sc, ^{45}Sc, ^{46}Sc, ^{47}Ti, ^{48}Sc, and ^{48}V using an $(f_{7/2})^n$ model and for transitions to ^{44}Sc, ^{45}Sc, ^{46}Sc, and ^{48}Sc using an $(f_{7/2}p_{3/2})^n$ model. Both models are based on an inert ^{40}Ca core. Zero-range distorted-wave Born-approximations calculations are then performed with these amplitudes. Reasonable agreement is found for the ratio of $L_{np} = 0+2$ to $L_{np} = 0$ strength with both models.

[NUCLEAR REACTIONS ^{43}Ca(^{3}He, p), ^{45}Sc(^{3}He, p), ^{46,48,50}Ti(^{3}He, p), $E = 17$ MeV; measured energy levels, $\sigma(\theta)$. Systematics of $\sigma(\theta)$ for $L_{np} = 0$ and $0+2$. Shell-model calculations.]

I. INTRODUCTION

Many (^{3}He, p) cross section measurements have been made with (fp)-shell nuclei and some systematics are beginning to emerge.[1] The present work is concerned with furthering our understanding of the systematics and comparing some of the experimental results with shell-model calculations. Only states populated by a transfer of 0 or $0+2$ units of orbital angular momentum (L_{np}) will be considered. Isobaric analog and antianalog states are populated by $L_{np} = 0$ while 1^+ states (for even-even targets) and $\frac{5}{2}^-$, $\frac{7}{2}^-$, or $\frac{9}{2}^-$ states (for the odd-A targets considered) are populated by $L_{np} = 0+2$. These transitions are easily found because the proton angular distributions display a characteristically sharp drop with increasing angle at forward angles. Data obtained using even-even (fp)-shell nuclei as targets showed that, although the number of states populated by $L_{np} = 0+2$ varies erratically, the sum of these cross sections has a systematic variation. Hansen and Nathan[1] stated that this sum is about the same for targets with empty p shells and diminishes as the p shell fills. They explain this trend by assuming that the major contribution to the cross sections comes from the p shell for all the (fp) targets. To investigate this further we decided to use the odd-A nuclei ^{43}Ca and ^{45}Sc as targets and to obtain the cross sections for $L_{np} = 0+2$. Results for the summed cross sections could then be compared with published data on even-even targets. To compare work from different laboratories it is usually necessary to make a normalization to account for different experimental conditions—such as the angles at which measurements are taken. For this reason we decided to repeat work we[2,3] and others[1,4] have done on targets of the even Ti isotopes. These results, obtained under the same experimental conditions as those used to obtain the cross sections for the odd-A targets, could then be used to normalize the odd-A data to the large amount of information on even-A targets summarized elsewhere.[1] In Sec. II a brief summary is given of the results for the even-Ti and ^{45}Sc targets, and detailed results are presented for the ^{43}Ca target.

When the sums of the cross sections for $L_{np} = 0+2$ were obtained for the two odd-A nuclei studied, they were found to be surprisingly low. To interpret these results we have calculated two-particle spectroscopic amplitudes on the basis of $f_{7/2}$ and $f_{7/2}p_{3/2}$ models. We have used these amplitudes to make distorted-wave Born-approximation (DWBA) calculations, concentrating

TABLE I. Isotopic abundances (in atomic percent) and total thicknesses of targets. The mass numbers refer to the target element.

Target	Mass number										Thickness
	40	42	43	44	45	46	47	48	49	50	(μg/cm^2)
^{43}Ca	12.78	0.65	81.12	5.40		<0.05		<0.05			235 ± 47
											112 ± 23
^{45}Sc					100						136 ± 28
^{46}Ti						84.4	4.8	9.6	0.6	0.7	232 ± 46
^{48}Ti						0.1	0.2	99.4	0.2	0.06	103 ± 21
^{50}Ti						1.4	1.3	11.8	3.5	82.0	169 ± 34

on comparing $L_{np} = 0 + 2$ and $L_{np} = 0$ strengths with the experimental results. The systematics of these results will be given in Sec. III.

II. EXPERIMENTAL PROCEDURES AND RESULTS

A. (^{3}He,p) reaction with ^{46,48,50}Ti and ^{45}Sc targets

The (^{3}He, p) reaction using $^{46, 48, 50}$Ti and ^{45}Sc targets was studied with the Argonne split-pole magnetic spectrograph.[5, 6] All targets were made by rolling Ti or Sc metal of the isotopic compositions given in Table I, which includes target thicknesses. A 17-MeV ^{3}He^{++} beam from the Argonne FN tandem Van de Graaff bombarded the target. The emergent protons were detected by Kodak NTB emulsions 50 μm thick which had been covered with acetate foils to stop particles produced in other reactions. After photographic development of the emulsions, the proton tracks were counted by an automatic nuclear-emulsion scanner.[7]

Table II gives cross sections for populating final states reached when the n-p pair transfers 0 or 0 + 2 units of angular momentum. Other cross sections are not given here because we limit our discussion to the systematics of $L_{np} = 0$ or 0 + 2. Results similar to those given in Table II have been published by others.[1, 4, 8] After making DWBA calculations[9] to take into consideration the different energies and angles used in other experiments, we found that our cross sections were about 30% lower, on the average, than those published by others. Most likely this discrepancy results from a combination of two causes. First, the compari-

TABLE II. Results for the (^{3}He,p) reaction on scandium and titanium targets. The states reported below are all populated by $L_{np} = 0+2$ except those indicated by footnotes which are populated by $L_{np} = 0$. A bombarding energy of 17 MeV was used and the cross sections are reported for a laboratory angle of 7°.

^{46}Ti target		^{48}Ti target		^{50}Ti target		^{45}Sc target	
E_x [a] (MeV)	$(d\sigma/d\omega)_{c.m.}$ [b] (μb/sr)	E_x [a] (MeV)	$(d\sigma/d\omega)_{c.m.}$ [b] (μb/sr)	E_x [a] (MeV)	$(d\sigma/d\omega)_{c.m.}$ [b] (μb/sr)	E_x [a] (MeV)	$(d\sigma/d\omega)_{c.m.}$ [b] (μb/sr)
0.421	54 ± 8	1.333	86 ± 12	0.141	160 ± 30	0.150	8 ± 2
2.289	182 ± 27	1.500	66 ± 10	1.294	105 ± 20	2.613	15 ± 2
2.408	69 ± 14	2.425	53 ± 8	1.666	305 ± 50	2.835	47 ± 8
3.019 [c]	409 ± 47	2.813	122 ± 22	2.106	43 ± 10	3.219 [d]	17 ± 2
3.702	268 ± 36	3.220	102 ± 22	2.151	110 ± 20	3.246	14 ± 2
3.866	416 ± 47	3.243	24 ± 5	2.396 [d]	145 ± 30	4.252	10 ± 2
4.698	210 ± 30	3.465	260 ± 35	2.591	487 ± 50	4.705	18 ± 3
4.798	98 ± 18	3.568 [d]	118 ± 17	3.556	101 ± 20	5.438	23 ± 4
		4.427	90 ± 15	4.628	96 ± 30	6.530	40 ± 7
		4.715	53 ± 8	8.829 [c]	368 ± 50	6.864	34 ± 8
		4.823 [c]	210 ± 31			7.370 [c]	280 ± 35
		5.759	51 ± 9			7.504	50 ± 8
		8.558 [c]	194 ± 27				

[a] The uncertainty in the excitation energies is ± 0.015 MeV.

[b] The uncertainties in the cross sections do not include a ± 20% contribution from the uncertainty in the target thicknesses.

[c] Isobaric analog state.

[d] Antianalog state.

son necessitates use of a set of optical-model parameters; thus if a different set were chosen, the extrapolated cross sections would change somewhat. Second, the measurements have systematic errors due to uncertainties in the target thicknesses. According to Hansen and Nathan[1] the absolute cross section scales are better than ±15% in the work they report. We measured the thicknesses of our targets both by Rutherford scattering experiments and by determining the energy loss of α particles going through the targets. These measurements agreed to better than 15% in all cases, and we have conservatively assigned a ±20% uncertainty to our target thicknesses.

It should be pointed out that while the present results for ^{48}V and ^{47}Ti are in good agreement with those we published earlier,[2,8] the present results for ^{50}V are considerably higher than those we have previously reported.[3] We believe the earlier measurements are incorrect, probably due to an error in the measurement of the target thickness.

B. (^{3}He,p) reaction with a ^{43}Ca target

The ^{43}Ca(^{3}He, p)^{45}Sc reaction was studied with equipment and under experimental conditions discussed in Sec. II A. The isotopic composition of the Ca targets used is given in Table I. Angular distributions ranging from 7 to 55° (laboratory angle) were taken with a Ca target 235 μg/cm^2 thick. In addition, proton spectra were taken at angles of 7, 9, 15, and 26° with a Ca target 112 μg/cm^2 thick. Measurements made with the former thickness resulted in an energy resolution [full width at half-maximum (FWHM)] of about 45 keV, while those made with the latter yielded a resolution of about 25 keV.

Figure 1 is the proton spectrum taken at an angle of 7° using the thin target. The excitation energies of peaks numbered in the figure are given in Table III. Proton groups caused by the (^{3}He, p) reaction on nuclei other than ^{43}Ca are labeled by the final nucleus with the excitation energy of the state populated given in brackets. Many of the major peaks are caused by the ^{40}Ca

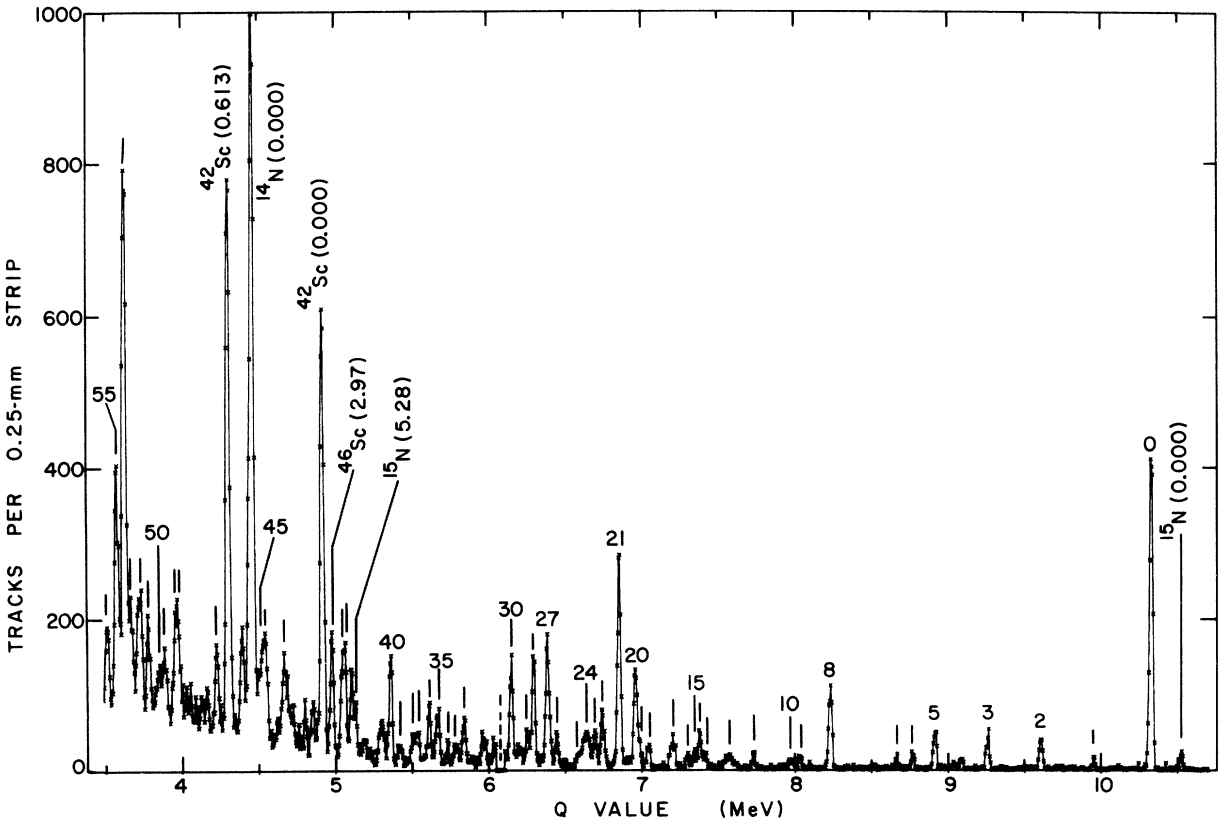

FIG. 1. Proton yield of the ^{43}Ca(^{3}He, p)^{45}Sc reaction as a function of Q value. The spectrum was obtained with the split-pole magnetic spectrograph at an angle of 7° to the incident 17-MeV ^{3}He^{++} beam. The proton groups numbered or indicated by a line correspond to states in ^{45}Sc and the excitation energies are listed in Table III. Nuclei reached by the (^{3}He, p) reaction on impurities are labeled, the number in parentheses giving the excitation energy in MeV.

TABLE III. Summary of excitation energies, maximum differential cross sections, and L_{np} values for some levels in ^{45}Sc.

Level No.	E_x [a] (MeV)	$(d\sigma/d\omega)^{max}_{c.m.}$ [b] (μb/sr)	L_{np}	Level No.	E_x [a] (MeV)	$(d\sigma/d\omega)^{max}_{c.m.}$ [b] (μb/sr)	L_{np}
0	0.000	92 ± 4	0+2	29	4.078	8 ± 1	(0 + 2)
1	0.376	4 ± 1	2	30	4.176	19 ± 2	(1, 0+2)
2	0.721	8 ± 1	0+2	31	4.240		
3	1.069	12 ± 1	2	32	4.488	19 ± 2	(1, 0+2)
4	1.240	4 ± 1		33	4.542		
5	1.414	12 ± 1	0+2	34	4.601		
6	1.559	10 ± 1	2	35	4.660	16 ± 1	(1, 0+2)
7	1.665	3 ± 1		36	4.716	15 ± 1	(1, 0+2)
8	2.095	18 ± 1	0+2	37	4.795		
9	2.295	6 ± 1	2	38	4.822		
10	2.351	4 ± 1	2	39	4.920	10 ± 1	2
11	2.600	4 ± 1		40	4.970	30 ± 3	0+2
12	2.759	13 ± 2	0+2	41	5.268	48 ± 3	
13	2.914			42	5.288		
14	2.950			43	5.661	29 ± 3	(1, 0+2)
15	2.989			44	5.786	39 ± 3	(1, 0+2)
16	3.031		(2)	45	5.824	23 ± 5	(1, 0+2)
17	3.125	11 ± 2	0+2	46	6.102	22 ± 2	
18	3.290	5 ± 1		47	6.344	54 ± 6	(0+2)
19	3.348			48	6.369		
20	3.367	21 ± 2	0+2	49	6.441		
21	3.473	53 ± 3	0+2	50	6.476		
22	3.581	17 ± 2	0+2	51	6.551	27 ± 4	0+2
23	3.636	10 ± 1	(1, 0+2)	52	6.609	42 ± 8	
24	3.696	15 ± 2		53	6.667	36 ± 8	(0+2)
25	3.730	10 ± 1		54	6.699	208 ± 20	0
26	3.883	8 ± 1		55	6.751	56 ± 6	(0+2)
27	3.938	36 ± 3	0+2	56	6.820	26 ± 3	0+2
28	4.034	27 ± 2	0+2				

[a] Levels from 1 through 15 inclusive have an uncertainty of ±0.010 MeV while the others have an uncertainty of ±0.015 MeV.

[b] The cross section uncertainties do not include a ± 20% contribution from the target thickness measurement.

in the target although its abundance is only 12.78%. Using the calibration for the magnetic spectrograph and the well-known Q value for the ^{12}C-(^{3}He, p)^{14}N (0.000-MeV) reaction we determined the Q value for the ^{40}Ca(^{3}He, p)^{42}Sc (0.000-MeV) reaction to be 4.904 ± 0.005 MeV, in good agreement with the value of 4.904 MeV calculated from atomic masses.[10] We obtained differential cross sections for the ^{40}Ca(^{3}He, p)^{42}Sc reaction, and results published earlier[11] agree with those in the present work. In addition, several of the proton groups are due to the (^{3}He, p) reaction with the ^{44}Ca in the target. The strongest is due to the isobaric analog of the ^{46}Ca ground state at an excitation energy of 5.03 MeV in ^{46}Sc. Our result for the cross section for populating this state at a laboratory angle of 7° and a bombarding energy of 17 MeV is 0.51 ± 0.03 mb/sr. This value agrees reasonably well with the value of 0.64 mb/sr reported by Schlegel *et al.*[11] at 5° and 18 MeV.

The angular distributions of protons leading to states in ^{45}Sc are given in Figs. 2–11. In this section we shall give the L_{np} assignments, deferring until Sec. III a comparison with DWBA calculations. Figures 2 and 3 show similar angular distributions, and since the 0.376-MeV state is known[12, 13] to have $J^\pi = \frac{3}{2}^-$ with a configuration $(2p_{3/2})^1(1f_{7/2})^4$, these states are populated by $L_{np} = 2$. The angular distribution of the isobaric analog of the ground state of ^{45}Ca is shown in Fig. 4, and is dominated by $L_{np} = 0$. Figures 5–9 are angular distributions in which transfers by 0 units of angular momentum and 2 units of angular momentum both contribute. These are characterized[14, 15] by a filling in of the deep minimum characteristic of an angular distribution due to a pure $L_{np} = 0$ transfer. Several angular distributions, shown in Figs. 10 and 11, are distinctly flatter at the forward angles than those assigned $L_{np} = 0 + 2$. Such angular distributions could signify

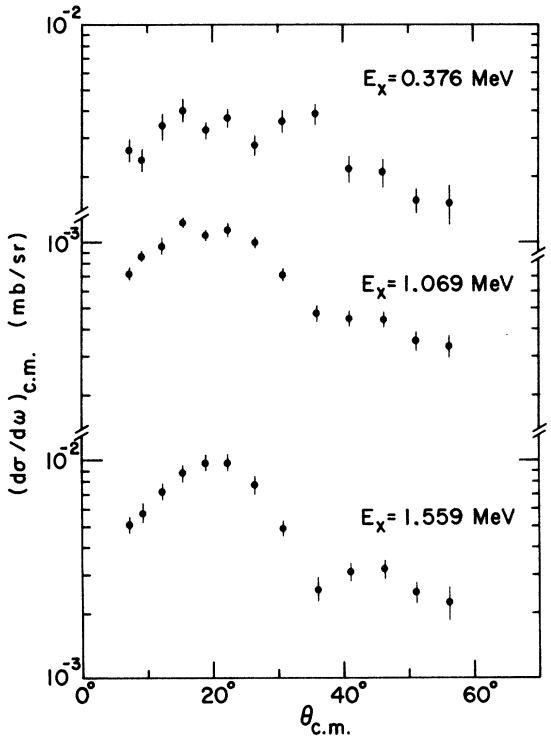

FIG. 2. Angular distributions of protons from the ^{43}Ca(^{3}He, p)^{45}Sc reactions with $L_{np} = 2$. The energy of the beam was 17 MeV.

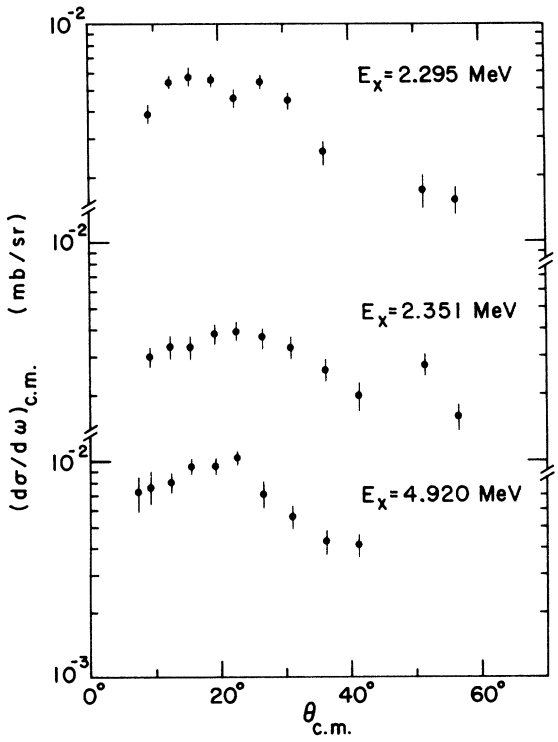

FIG. 3. Same as Fig. 2.

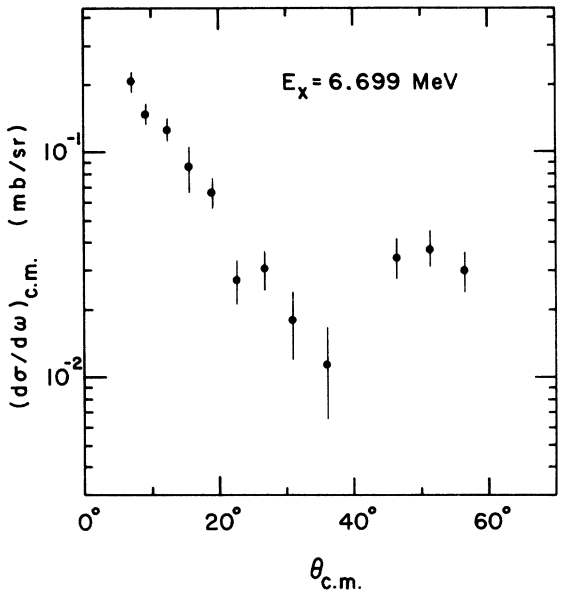

FIG. 4. Angular distribution of protons from the ^{43}Ca(^{3}He, p)^{45}Sc reaction with $L_{np} = 0$. The energy of the beam was 17 MeV.

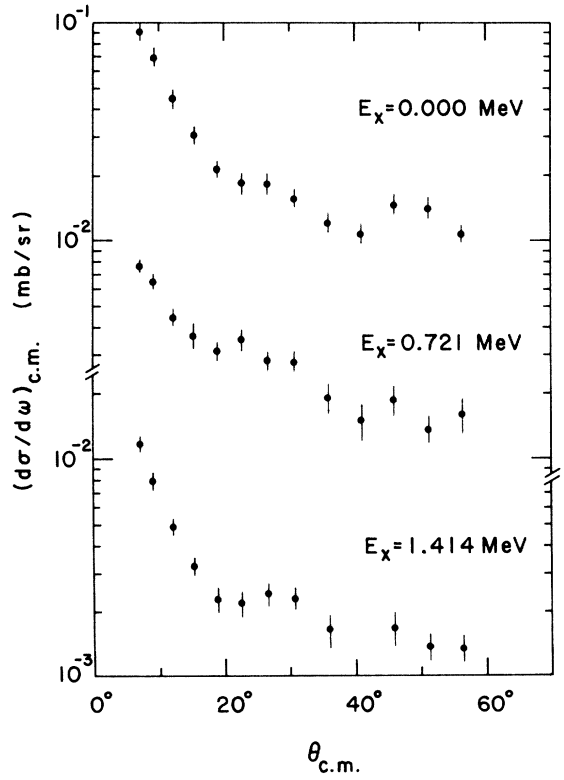

FIG. 5. Angular distributions of protons from the ^{43}Ca(^{3}He, p)^{45}Sc reaction with $L_{np} = 0 + 2$. The energy of the beam was 17 MeV.

$L_{np} = 1$ or that several L_{np}'s are making significant contributions (see Sec. III B). It should be emphasized that these distributions, which are very much alike, are distinctly different from those assigned $L_{np} = 0 + 2$, and there is no smooth transition between these two classes of shapes. An $L_{np} = 0 + 2$ assignment for the angular distributions in Figs. 10 and 11 is therefore somewhat unlikely, but certainly not ruled out.

Our results agree quite well with those in an earlier study of the ^{43}Ca(^{3}He, p)^{45}Sc reaction by Schlegel *et al.*[11] The only major disagreements concern states at 4.72 and 5.28 MeV which, according to Schlegel *et al.*,[11] are relatively intense and populated by pure $L_{np} = 0$. We observe a state with $E_x = 4.716$ MeV whose yield decreases with increasing angle much more slowly than an $L_{np} = 0$ distribution. This shape could result from two closely spaced proton groups. Indeed, Schlegel *et al.*[11] report a state in ^{46}Sc with $E_x = 2.37$ MeV, and the proton group populating this state (due to the presence of ^{44}Ca in the target) should be very close to the proton group resulting from the population of the 4.716-MeV state. In the excitation energy region around 5.28 MeV we observe two states (5.268 and 5.288 MeV) but are not able to resolve them sufficiently to extract their separate angular distributions.

Unfortunately, because the spin of the target is $\frac{7}{2}$, the L_{np} values obtained in the present experiment do not permit unique spin assignments for the final states. An $L_{np} = 0 + 2$ indicates a J^π of $\frac{5}{2}^-$, $\frac{7}{2}^-$, or $\frac{9}{2}^-$ while states with J^π from $\frac{1}{2}^-$ to $\frac{13}{2}^-$ could be populated by $L_{np} = 2$. However, it has been found experimentally for fp-shell nuclei, that when $L_{np} = 2$ occurs, one nucleon goes into the $f_{7/2}$ shell and the other into the p shell, and the states populated have either $J^\pi = \frac{1}{2}^-$ or $\frac{3}{2}^-$.

The present assignments of the angular momentum transfer can be compared with the results of other experiments, particularly the one-nucleon transfer reactions. The ^{46}Ti(d, ^{3}He)^{45}Sc reaction has been studied by Ohnuma[13] while Schwartz and Alford[12] have studied the ^{44}Ca(^{3}He, d)^{45}Sc reaction. States formed by the stripping or pickup of a proton with $l_p = 3$ should be produced by $L_{np} = 0 + 2$ in the present experiment, both particles going in the f shell. This is the case, and Table IV[16, 18-20] summarizes the results of the one-nucleon transfer reactions, along with some of our results, and gives the spin and parity assignments. Also, the $l_p = 1$ transitions observed in the one-nucleon transfer reactions should be observed by

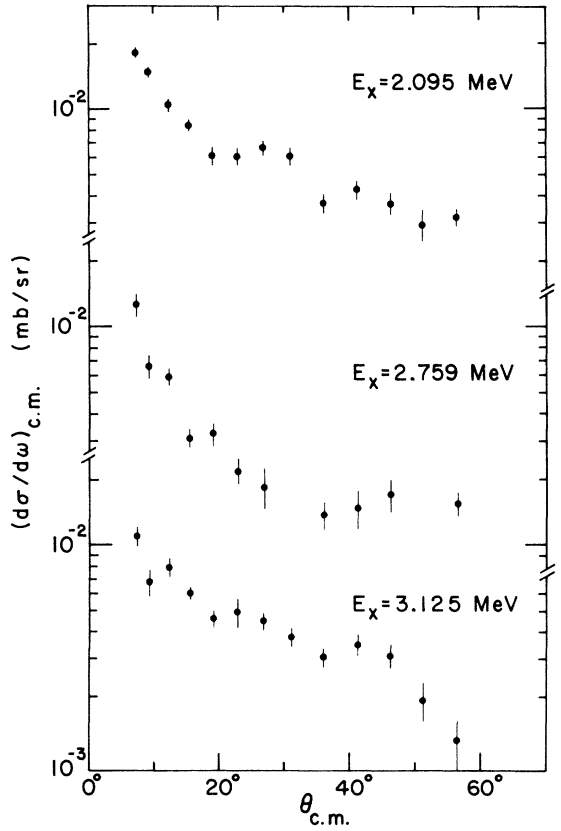

FIG. 6. Same as Fig. 5.

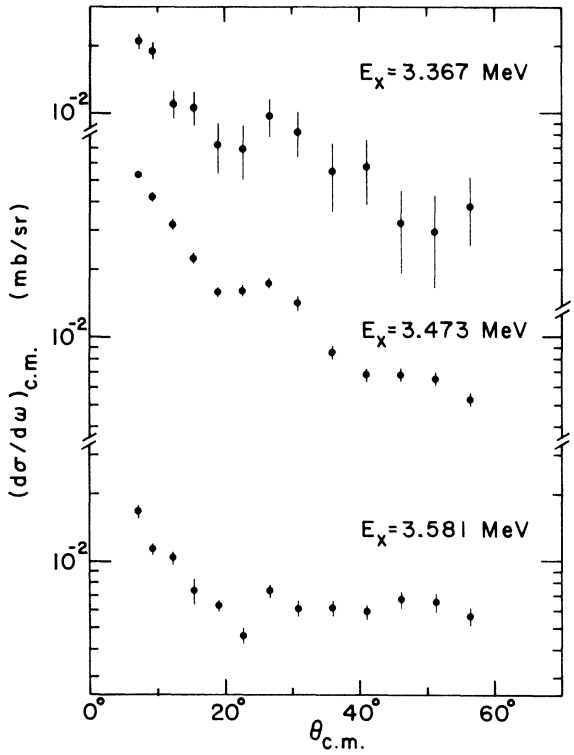

FIG. 7. Same as Fig. 5.

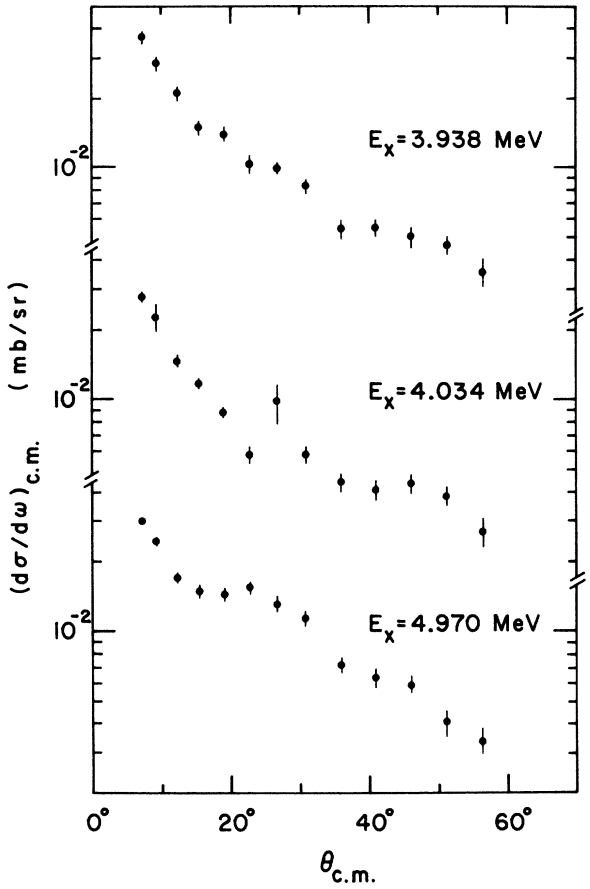

FIG. 8. Same as Fig. 5.

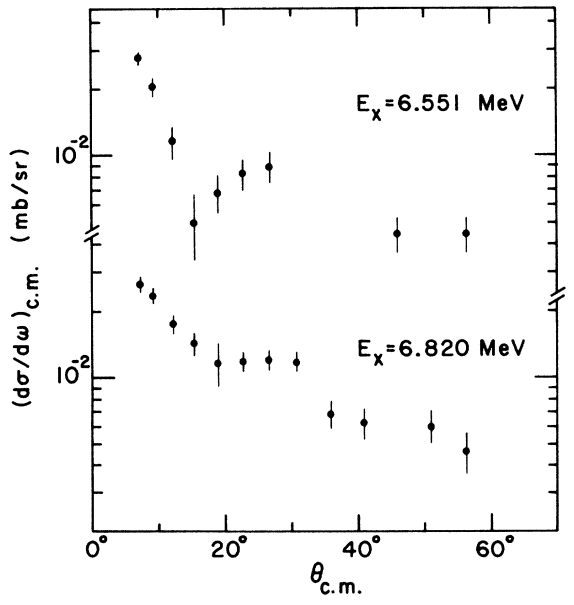

FIG. 9. Same as Fig. 5.

us as $L_{np}=2$ transitions with one nucleon going into the p shell and the other into the $f_{7/2}$ shell. Again reference to Table IV shows that this association between l_p and L_{np} is generally the case. In the two cases of disagreement (levels to which we have assigned excitation energies of 3.473 and 3.938 MeV) there are probably two closely spaced levels, one member of each set being populated in the (^{3}He, p) reaction and the other member by the one-nucleon transfer reaction. No low-lying even-parity states have been observed in the (^{3}He, d) or (^{3}He, p) reactions.

C. Summary of $L_{np}=0$ and $0+2$ transition strength to f-shell targets

Figure 12 is a rough summary of differential cross sections for populating states by $J^{\pi}{}_{np}=1^+$ with both even-even and odd-A $f_{7/2}$ shell targets from ^{40}Ca to ^{50}Ti. (Dotted lines show the cross

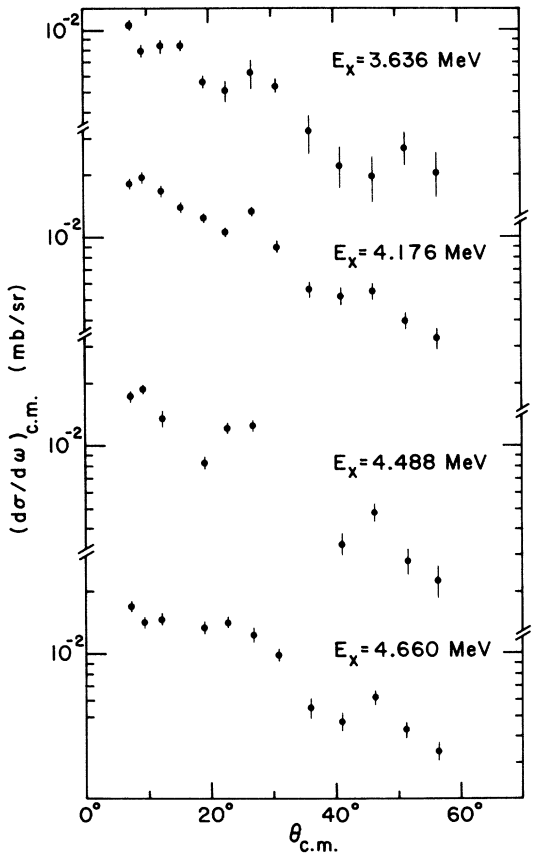

FIG. 10. Angular distributions of protons from the ^{43}Ca(^{3}He, p)^{45}Sc reaction whose L_{np} assignment is uncertain. The energy of the beam was 17 MeV. Possible assignments for these distributions are $L_{np}=1$ or $L_{np}=0+2$ but with higher components (4, 6) contributing significantly.

sections for $J^{\pi}_{np} = 0^+$ to isobaric analogs of the ground states of the parent nuclei.) The cross sections have been measured at bombarding energies ranging from 15 to 18 MeV. The data have been taken at a laboratory angle of 7° or have been normalized to this angle. Much of the work has been done at 3.75° (see Table V[1, 8, 11, 21-27]) and these cross sections have been divided by 1.8 to normalize them to 7°. This factor was obtained by comparing our cross section data on even-even targets with those given by Hansen and Nathan.[1] In some instances it was necessary to use information from two sources to obtain absolute cross sections. For example, the absolute cross section for the isobaric analog state in ^{48}Sc was obtained by combining the relative cross section measurements for populating $J^{\pi} = 1^+$ and 0^+ states made by Fleming *et al.*[17] with the absolute cross sections for populating 1^+ states given by Hansen and Nathan.[1]

In Sec. III the cross sections for $L_{np} = 0$ transitions and the sum of the cross sections for $L_{np} = 0 + 2$ transitions will be discussed. These cross sections are summarized in Table V.

III. DISCUSSION

A. Shell-model calculations

There do not exist nuclear structure models for the $f_{7/2}$ shell that adequately describe details of the (^{3}He, p) strength observed in experiments. Since very low-lying positive-parity states exist in the odd-A, $f_{7/2}$-shell nuclei we expect that a fully successful model would include both the (fp) shells and excitation from the (ds) shells. Shell-model calculations of this complexity would be enormous in size and expense. We have, therefore, severely limited our models and attempted to account for only the simplest features of the (^{3}He, p) data.

Results from two nuclear-structure models will be compared with experimental data. Both models assume ^{40}Ca to be an inert core. The first model

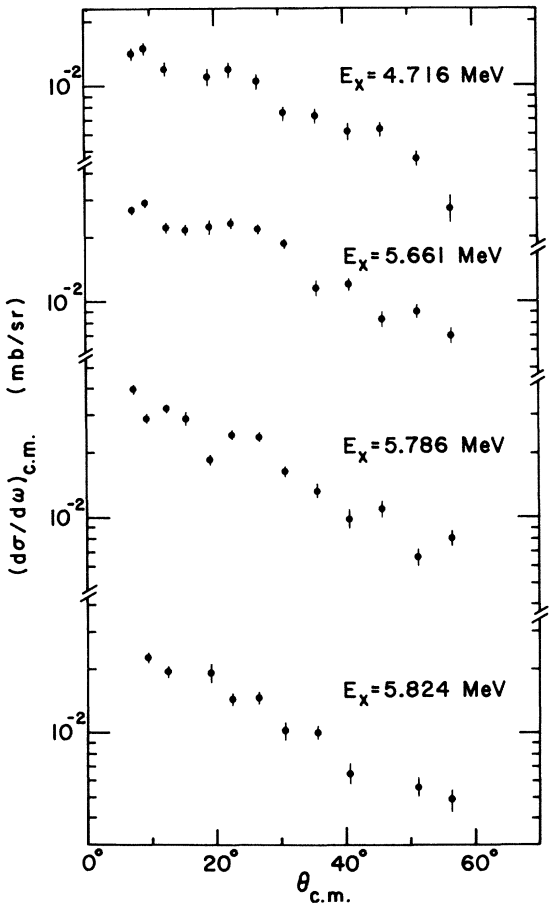

FIG. 11. Same as Fig. 10.

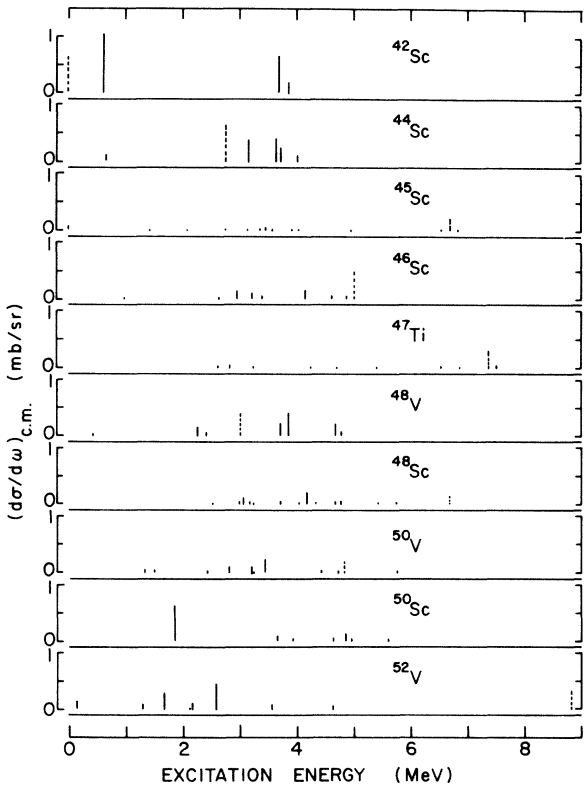

FIG. 12. A summary of (^{3}He, p) reactions leading to the final nuclei given in the figure. The solid lines show the cross sections for $L_{np} = 0 + 2$ and the dashed lines show the cross sections for populating the isobaric analog states. The data have either been taken at an angle of 7° (laboratory) or normalized to that angle (see Sec. II C).

TABLE IV. Comparison of some of the results of the present (^{3}He,p) experiment with one-nucleon transfer reactions. A summary of spins and parities is also given.

^{46}Ti(d,^{3}He)^{45}Sc Ref. 13		^{44}Ca(^{3}He,d)^{45}Sc Ref. 12		^{43}Ca(^{3}He,p)^{45}Sc Present work			
E_x (MeV)	l_p	E_x (MeV)	l_p	E_x (MeV)	L_{np}	J^π	Comments on J^π
0.000	3	0.000	3	0.000	0+2	$\frac{7}{2}^-$	
0.012	2					$\frac{3}{2}^+$	
0.381	1	0.378	1	0.376	2	$\frac{3}{2}^-$	
0.543	2					$\frac{5}{2}^+$	
0.726	3			0.721	0+2	$\frac{5}{2}^-$	
0.943	0					$\frac{1}{2}^+$	
1.067	1	1.067	1	1.069	2	$\frac{3}{2}^-$	
1.235				1.240		$\frac{11}{2}^-$	From (α,p): Ref. 16
1.304	2					$\frac{3}{2}^+$	
1.417	(3)			1.414	0+2	$\frac{7}{2}^-$	From (p,$p'\gamma$): Ref. 18
1.556	1	1.553	1	1.559	2	$\frac{1}{2}^-$	
				1.665		$\frac{9}{2}^-$	From (α,p): Ref. 16
1.799	2					$\frac{5}{2}^+$	
				2.095	0+2		
				2.295	2	$(\frac{1}{2}, \frac{3}{2})^-$	
		2.349	1	2.351	2	$(\frac{1}{2}, \frac{3}{2})^-$	From (p,p'): Ref. 19
		2.75	3	2.759	0+2	$\frac{7}{2}^-$	See Ref. 12
		2.980	1	2.989		$\frac{3}{2}^-$	From (α,p): Ref. 20
		3.022	1	3.031	(2)	$(\frac{1}{2}, \frac{3}{2})^-$	
				3.125	0+2	$(\frac{5}{2}, \frac{7}{2}, \frac{9}{2})^-$	
				3.367	0+2	$(\frac{5}{2}, \frac{7}{2}, \frac{9}{2})^-$	
		3.407	1			$(\frac{1}{2}, \frac{3}{2})^-$	
		3.484	1	3.473	0+2	$(\frac{5}{2})^-$	From (α,p): Ref. 20
				3.581	0+2	$(\frac{5}{2}, \frac{7}{2}, \frac{9}{2})^-$	
		3.724	1	3.730		$(\frac{1}{2}, \frac{3}{2})^-$	
		3.881	1	3.883		$(\frac{1}{2}, \frac{3}{2})^-$	
		3.926 [a]	1	3.938 [a]	0+2		
				4.034	0+2	$(\frac{5}{2}, \frac{7}{2}, \frac{9}{2})^-$	
		4.505	1	4.078	(0+2)	$(\frac{5}{2}, \frac{7}{2}, \frac{9}{2})^-$ $(\frac{1}{2}, \frac{3}{2})^-$	
				4.920	2	$(\frac{1}{2}, \frac{3}{2})^-$	
				4.970	0+2	$(\frac{5}{2}, \frac{7}{2}, \frac{9}{2})^-$	
				6.551	0+2	$(\frac{5}{2}, \frac{7}{2}, \frac{9}{2})^-$	
				6.667	(0+2)	$(\frac{5}{2}, \frac{7}{2}, \frac{9}{2})^-$	
				6.699	0	$\frac{7}{2}^-$	
				6.751	(0+2)	$(\frac{5}{2}, \frac{7}{2}, \frac{9}{2})^-$	
				6.820	0+2	$(\frac{5}{2}, \frac{7}{2}, \frac{9}{2})^-$	

[a] Probably two levels.

TABLE V. The sum of the differential cross sections for all states reached by $L_{np}=0+2$. Also given are the cross sections for populating the isobaric analogs of the ground states of the parent nuclei. The data were either taken at, or normalized to, a laboratory angle of 7°.

Final nucleus	$\sum(d\sigma/d\omega)_{c.m.}$ (mb/sr)	$(d\sigma/d\omega)_{c.m.}$ (IAS) (mb/sr)
^{42}Sc	1.91 [a]	0.61 [b]
^{44}Sc	1.34 [a]	0.66 [c]
^{45}Sc	0.39–0.71 [d,e]	0.21 [d]
^{46}Sc	0.78 [a]	0.51 [d]
^{47}Ti	0.26 [d]	0.32 [f]
^{48}Sc	0.93 [a]	0.15 [g]
^{50}Sc	1.16 [a]	0.21 [h]
^{48}V	1.30 [d]	0.41 [d]
^{50}V	0.91 [d]	0.21 [d]
^{52}V	1.41 [d]	0.37 [d]
^{52}Mn	1.16 [a]	0.24 [i]
^{54}Mn	1.55 [a]	0.54 [j]
^{56}Mn	0.76 [a]	
^{56}Co	1.15 [a]	
^{58}Co	0.88 [a]	0.32 [k]
^{60}Co	0.41 [a]	

[a] From Ref. 1.
[b] From Ref. 21.
[c] From Ref. 11.
[d] From present work.
[e] See Sec. II B.
[f] From Ref. 8.
[g] From Refs. 22 and 1.
[h] From Refs. 11 and 23.
[i] From Refs. 24 and 1.
[j] From Ref. 25.
[k] From Refs. 26 and 27.

TABLE VI. Two-body matrix elements of the form $\langle f_{7/2}f_{7/2}|V_{\text{eff}}|f_{7/2}f_{7/2}\rangle$, deduced from the experimental energy-level spectrum of ^{42}Sc.

J	T	Value of matrix element (keV)
0	1	0.000
1	0	0.615
2	1	1.593
3	0	1.498
4	1	2.800
5	0	1.518
6	1	3.200
7	0	0.625

limits active nucleons to the $f_{7/2}$ shell. Two-body matrix elements, given in Table VI, are obtained[28] from the spectrum of ^{42}Sc. The second model permits active nucleons in both the $f_{7/2}$ and $p_{3/2}$ shells. The effective interaction for this second model was that obtained by McGrory and Halbert[29] from a fit to a set of low-lying states in the $A=42$ to 44 nuclei. These states were calculated using Kuo-Brown[30] matrix elements for the full (fp) shell. The two-body matrix elements are given in Table VII. The calculations for the two models were performed using the Argonne nuclear shell-model codes.[31]

In our comparison between theory and experiment we shall consider only the strongest (^{3}He, p) transitions, namely those to analog states and those of $L_{np}=0+2$ type (i.e., to 1^+ states in even-A nuclei, and $\frac{5}{2}^-$, $\frac{7}{2}^-$, or $\frac{9}{2}^-$ in odd-A nuclei). All the DWBA calculations have been performed using the zero-range code TWOPAR with the optical-model parameters given in Table VIII. This code was written for a reaction $A(^3\text{He}, p)B$ with the differential cross section in the form [see, e.g. Eq. (2.61) in Ref. 32]

$$\frac{d\sigma}{d\omega} \propto \sum_{LSJT} \left[b_{ST} C \begin{matrix} T_B & T & T_A \\ (T_z)_B & [(T_z)_A-(T_z)_B] & (T_z)_A \end{matrix} D(S,T) \right]^2 \left| \sum_\gamma \beta^\gamma_{LSJ} S^\gamma_J \right|^2 ,$$

where b_S is the spectroscopic amplitude for the light particles. (Each pair of nucleons in ^{3}He and the transferred pair are assumed to be in relative s states.) The symbol

$$C \begin{matrix} T_B & T & T_A \\ (T_z)_B & [(T_z)_A-(T_z)_B] & (T_z)_A \end{matrix}$$

represents the isospin Clebsch-Gordan coefficient connecting the target, transferred pair, and residual nucleus. The symbol β^γ_{LSJ} represents a transition amplitude for the transfer of a pair of nucleons with orbital angular momentum L, spin S, and total angular momentum J. The symbol S^γ_J represents the spectroscopic amplitude for the transfer of a pair of nucleons coupled to J between the initial state A and final state B. In the present case the superscript γ refers to the transfer of a pair of nucleons into the $f_{7/2}$ shell or into the $p_{3/2}$ shell. (There is only one term in the sum over γ in the $f_{7/2}$ model calculations.) The effect of coherent contributions from different L values, due to a spin-orbit term in the optical-model potential, has been found to be small[1,33] and is not considered in the present calculations. Since we

TABLE VII. Two-body matrix elements obtained from McGrory and Halbert.

Matrix element	J	T	Value of matrix element (keV)
$\langle f_{7/2} f_{7/2} \lvert V_{\text{eff}} \rvert f_{7/2} f_{7/2} \rangle$	0	1	−2.75
	1	0	−2.71
	2	1	−1.04
	3	0	−1.55
	4	1	−0.36
	5	0	−1.04
	6	1	0.20
	7	0	−2.47
$\langle f_{7/2} f_{7/2} \lvert V_{\text{eff}} \rvert f_{7/2} p_{3/2} \rangle$	2	1	−0.72
	3	0	−0.48
	4	1	−0.38
	5	0	−0.92
$\langle f_{7/2} f_{7/2} \lvert V_{\text{eff}} \rvert p_{3/2} p_{3/2} \rangle$	0	1	−1.22
	1	0	−0.28
	2	1	−0.58
	3	0	−0.30
$\langle f_{7/2} p_{3/2} \lvert V_{\text{eff}} \rvert f_{7/2} p_{3/2} \rangle$	2	0	−0.60
	2	1	−1.03
	3	0	−0.60
	3	1	−0.17
	4	0	−0.70
	4	1	−0.19
	5	0	−2.77
	5	1	0.15
$\langle f_{7/2} p_{3/2} \lvert V_{\text{eff}} \rvert p_{3/2} p_{3/2} \rangle$	2	1	−0.58
	3	0	−0.51
$\langle p_{3/2} p_{3/2} \lvert V_{\text{eff}} \rvert p_{3/2} p_{3/2} \rangle$	0	1	−1.72
	1	0	−0.64
	2	1	−0.64
	3	0	−1.83

assume the transferred particles are in a relative s state, the parity change in the reaction is related to L_{np} by $\Delta\pi = (-1)^{L_{np}}$. We are considering only transitions with no parity change and are therefore restricted to even values of L_{np}. For the (^{3}He, p) reaction the n-p may be transferred in an $S=0$, $T=1$ state, or in an $S=1$, $T=0$ state. The values for L_{np} and J_{np} that must be included in the differential cross section sum are listed in Table IX. Transfer of the two nucleons into the $2p_{3/2}$ shell of the $1f_{7/2}$ shell is labeled p-p and f-f, respectively.

The factor $D(S, T)$ in the above equation contains the spin and isospin dependence of the interaction potential. Towner and Hardy[32] have shown that

$$\left|\frac{D(0,1)}{D(1,0)}\right|^2 = \left|\frac{1-0.5(B+H)}{1-1.5(B+H)}\right|^2 = W ,$$

where B and H are the Bartlett and Heisenberg exchange terms in the interaction potential. Empirical fits[21, 33-35] have favored values of W near 2 or 3. We will compare calculations for both $W=1$ (no spin dependence and so $B=H=0$) and $W=3$.

B. Comparison of calculations with experimental results: Transitions to the scandium isotopes

The shell model should be best able to predict the strongest spectroscopic amplitudes. Among the strongest transitions in the (^{3}He, p) reaction are those to isobaric analog states. These states have large overlaps, and hence large spectroscopic amplitudes, with two nucleons in a $J=0$ state coupled to the target ground state. They are populated via the favored $L=0$ reaction amplitude. Other states strongly excited in the (^{3}He, p) reaction are some 1^+ states (even-even targets) and some $\frac{5}{2}^-$, $\frac{7}{2}^-$, and $\frac{9}{2}^-$ states (odd-A nuclei).

TABLE VIII. The optical potentials and parameters used in the DWBA calculations, in which the potential for the unbound proton or ^{3}He is

$$V(\boldsymbol{r}) = -Vf_v(\boldsymbol{r}) - iWf_w(\boldsymbol{r}) + 4ia_s W_s f_s'(\boldsymbol{r}) ,$$

where

$$f_x = \{1 + \exp[(r - r_x A^{1/3})/a_x]\}^{-1}$$

and $f' = \partial f/\partial r$. The parameters of the potential in which the bound neutron and proton move are $a_v = 0.65$ fm and $r_v = 1.25$ fm. The program adjusts the real potential well until the binding energy is $\boldsymbol{E} = \frac{1}{2}[|S_{np}| - E_x]$, where E_x is the excitation energy in the final nucleus and S_{np} is the separation energy of the n-p pair.

Unbound particle	V (MeV)	a_v (fm)	r_v (fm)	W (MeV)	a_w (fm)	r_w (fm)	W_s (MeV)	a_s (fm)	r_s (fm)
P	53.0	0.600	1.220	0.00	···	···	15.0	0.310	1.26
^{3}He	160.0	0.700	1.220	20.00	0.700	1.220	0.0	···	···

TABLE IX. Values of S, T, L_{np}, and J_{np} that must be considered in calculating the cross sections for various transitions.

Transition	S,T	L_{np} p-p	L_{np} f-f	J_{np} p-p	J_{np} f-f
$0^+ \rightarrow 0^+$	0,1	0	0	0	0
$0^+ \rightarrow 1^+$	1,0	0,2	0,2	1	1
$\frac{7}{2}^- \rightarrow \frac{7}{2}^-$	0,1	0,2	0,2,4,6	0,2	0,2,4,6
	1,0	0,2	0,2,4,6	1,3	1,3,5,7
$\frac{7}{2}^- \rightarrow \frac{5}{2}^-$	0,1	2	2,4,6	2	2,4,6
$\frac{9}{2}^-$	1,0	0,2	0,2,4,6	1,3	1,3,5,7

All these states are populated by $L_{np} = 0 + 2$. Since we are using a zero-range reaction code we cannot expect to predict absolute cross sections. Hence we shall first compare the summed strength leading to 1^+ states or $\frac{5}{2}^-$, $\frac{7}{2}^-$, or $\frac{9}{2}^-$ states with the strength to the isobaric analog state.

The ratios of the summed $L_{np} = 0 + 2$ strength to the analog strength, for even-even targets, are given in columns 2 to 6 (rows 1 to 3) of Table X. The experimentally determined ratios are similar for transitions to ^{44}Sc and ^{46}Sc, but are more than three times this value for ^{48}Sc. Both the $f_{7/2}$ model (columns 3 and 4) and $f_{7/2}p_{3/2}$ model (columns 5 and 6) predict this trend, although not enough $L_{np} = 0 + 2$ strength relative to the $L_{np} = 0$ strength is predicted for ^{48}Sc. Also in both models the experimental ratios lie close to the calculations with $W = 1$, thus favoring no significant exchange terms in the interaction potential.

While the predicted ratio of the sum of the $L_{np} = 0 + 2$ strength to the $L_{np} = 0$ strength is about the same in both models, the details of the distribution of strength are not. A striking illustration is found for transitions to ^{48}Sc. In this case the $f_{7/2}$ model is certainly inadequate to describe the 1^+ states since only one is predicted, though more than a dozen are seen[22] below the analog state. The $f_{7/2}p_{3/2}$ model, on the other hand, predicts 15 states with $J^\pi = 1^+$ below the analog.

Now we turn to a discussion of the ^{43}Ca(^{3}He, p)-^{45}Sc reaction. Many spectroscopic amplitudes may contribute in (^{3}He, p) transitions on odd-A targets (see Table IX). For transitions to $\frac{7}{2}^-$ states in ^{45}Sc, however, by far the most important spectroscopic amplitudes affecting the cross sections at forward angles are those for which the pair is coupled to $J_{np} = 0$ or 1, allowing $L_{np} = 0$ or 2. This is not true for some transitions (generally weak) with small spectroscopic amplitudes for $J_{np} = 0$ and 1 that are dominated at forward angles by the $L_{np} = 2$, 4, or 6 transition amplitudes. Again, transitions of strong and moderate strength to $\frac{5}{2}^-$ or $\frac{9}{2}^-$ states in ^{45}Sc are dominated at forward angles by the $J_{np} = 1$ spectroscopic amplitude ($L_{np} = 0$ and 2 transition amplitudes). The ratio of the summed $L_{np} = 0 + 2$ strength to the analog strength is given in the last row of Table X. The summed strength includes $J_{np} = 1$ transitions to all $\frac{5}{2}^-$ and $\frac{9}{2}^-$ bound model states and $J_{np} = 0$ and 1 transitions to bound $\frac{7}{2}^-$ states. If all possible L_{np} were included the ratios would be increased by about 10%.

The ratios are again quite similar in the $f_{7/2}$ model (columns 3 and 4 of Table X) and the $f_{7/2}p_{3/2}$ model (columns 5 and 6). It is difficult to compare these ratios with the experimental results because it is uncertain whether some or all of 12 states (see Table III and Sec. II B) should be assigned $L_{np} = 0 + 2$. The lower limit of 1.9 given in Table X includes all transitions positively identified as $L_{np} = 0 + 2$. If one includes the additional 12 transitions, the upper limit of 3.4 is obtained. The distribution of strength to $\frac{5}{2}^-$, $\frac{7}{2}^-$, and $\frac{9}{2}^-$ states is presented in Fig. 13. The $f_{7/2}p_{3/2}$ model predicts many more states than are observed and too much strength at higher energies. In fact this model predicts that over 50% of the strength is between 5 MeV and the isobaric analog state while the experimental results show only a

TABLE X. The experimentally determined $L_{np} = 0$ strength and its ratio with the experimentally determined sum of the $L_{np} = 0 + 2$ strengths compared with the calculations. The experimental values are from Table V($\theta = 7°$). In the calculations, transitions to all predicted bound states were included.

Reaction	$\left[\sum \frac{d\sigma}{d\omega}(L_{np}=0+2)\right] \Big/ \frac{d\sigma}{d\omega}(L_{np}=0)$ Exp.	f model $W=1$ [a]	f model $W=3$	fp model $W=1$	fp model $W=3$	$\frac{d\sigma}{d\omega}(L_{np}=0)$ Exp. (mb/sr)	Exp./Th.(fp) $W=3$	Th.(fp)/Th.(f) $W=3$
^{42}Ca(^{3}He,p)^{44}Sc	2.0	1.7	0.58	2.3	0.75	0.66	240	2.6
^{44}Ca(^{3}He,p)^{46}Sc	1.5	1.9	0.65	2.9	0.96	0.51	280	3.1
^{46}Ca(^{3}He,p)^{48}Sc	6.1	3.6	1.2	3.5	1.2	0.15	130	4.4
^{43}Ca(^{3}He,p)^{45}Sc	1.9 → 3.4 [b]	3.2	1.5	3.9	2.3	0.21	120	2.6

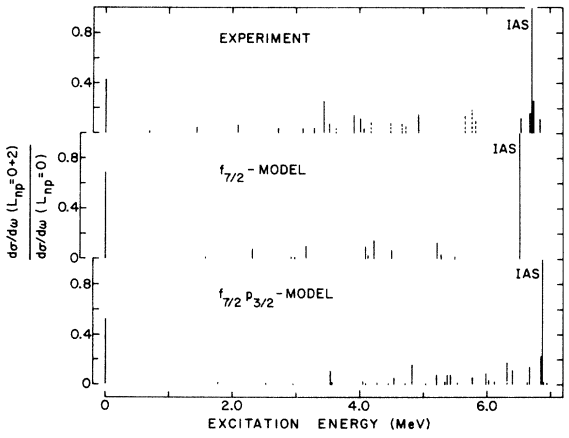

FIG. 13. A comparison of the experimentally determined distribution of $L_{np}=0+2$ strength with calculations, for the ^{43}Ca(^{3}He, p)^{45}Sc reaction. The differential cross sections for $L_{np}=0+2$ have been divided by the differential cross section for populating the isobaric analog of the ground state of ^{45}Ca. Included in the experimental results are four states for which the $L_{np}=0+2$ assignment is uncertain (see Table III). The eight dashed lines are for states whose natures are uncertain (see the discussion in Sec. II B) but may be populated by $L_{np}=0+2$.

few transitions with $L_{np}=0+2$ in this region. Since the experimentally determined ratio is quite uncertain it is not possible to decide which value for W is favored.

Another check on the calculations is to see how well they fit the observed proton angular distributions. However, a detailed comparison of angular distributions is hampered by the difficulty in making correspondences between the observed and model states (see Fig. 13). In fact the correspondence is obvious for only the ground and isobaric analog states.

The angular distribution for populating the ground state is given in Fig. 14. The curves presented were calculated with the $f_{7/2}$ model. The dashed curve is the result obtained when only $J_{np}=1$ is permitted while the other two curves are for $J_{np}=0$ to 7 (dot-dash curve for $W=1$ and solid curve for $W=3$). The curve for $J_{np}=1$ is seen to be a poor approximation to the full curve, except at angles less than 10°. The calculations with all the permissable J_{np}'s included predict relatively higher cross sections at larger angles than are observed. In a study of the comparison between the experimental angular distributions assigned $L_{np}=0+2$ and the angular distributions predicted

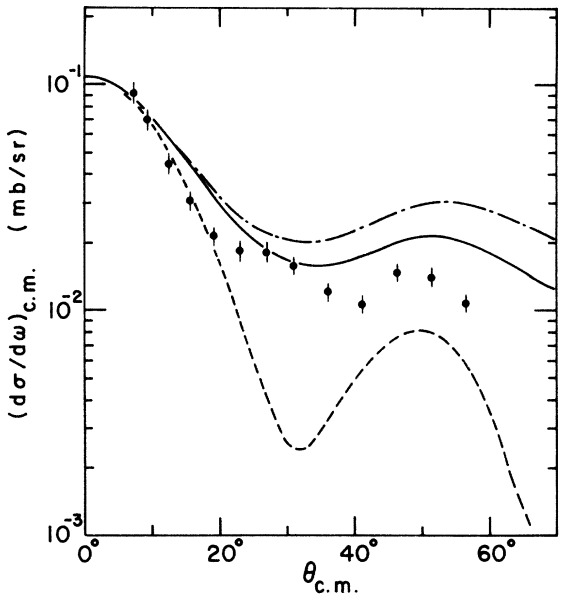

FIG. 14. A comparison of the angular distribution of protons populating the ground state of ^{45}Sc with calculations using the $f_{7/2}$ shell model. The dashed curve is the result if the calculations are restricted to $J_{np}=1$ ($L_{np}=0+2$). The other curves result when all possible J_{np} values are permitted, the solid and dot-dash curves are for $W=3$ and 1, respectively. The solid curve is normalized to the data and the other two curves are normalized to the solid curve at 0°.

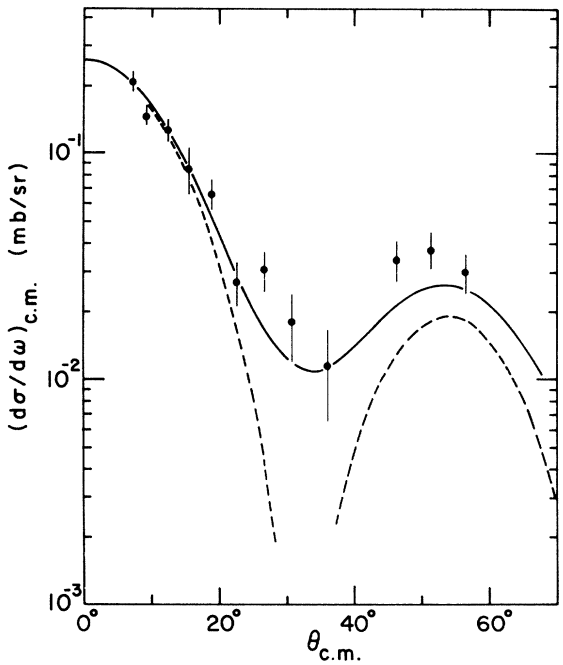

FIG. 15. A comparison of the angular distribution of protons populating the isobaric analog state at $E_x=6.699$ MeV, with calculations using the $f_{7/2}$ shell model. The dashed curve is the result if the calculations are restricted to $J_{np}=0$ ($L_{np}=0$). The solid curve results when all possible J_{np} values are permitted. The curves have been normalized to the data at forward angles.

TABLE XI. The experimentally determined $L_{np}=0$ strength and its ratio with the experimentally determined sum of the $L_{np}=0+2$ strengths compared with the results of calculations with the $f_{7/2}$ model. The experimental values are from Table V ($\theta=7°$). In the shell-model calculations, transitions to all predicted bound states are included.

Reaction	$\left[\sum \frac{d\sigma}{d\omega}(L_{np}=0+2)\right] / \frac{d\sigma}{d\omega}(L_{np}=0)$			$\frac{d\sigma}{d\omega}(L_{np}=0)$	
	Exp.	$f_{7/2}$ model		Exp.	Exp./Th. ($f_{7/2}$)
		$W=1$ [a]	$W=3$	(mb/sr)	$W=3$
^{45}Sc(^{3}He,p)^{47}Ti	0.81	2.0	0.78	0.32	440
^{46}Ti(^{3}He,p)^{48}V	3.2	1.5	0.50	0.41	480

[a] W is defined and discussed in Sec. III A.

for the stronger model states, this seems to be usually true. Hence, the calculations predict contributions from higher J_{np} values that are too large.

The angular distribution to the isobaric analog of the ground state of ^{45}Ca is given in Fig. 15. Again the angular distribution predicted when only $J_{np}=0$ is permitted has a deep minimum at about 35° which is filled in when all possible J_{np} values are included. In this case the agreement between the theoretical calculations with the $f_{7/2}$ model and the experimental results is excellent.

C. Normalization of the DWBA cross sections

Column 7 in Table X gives the experimentally determined differential cross sections at 7° (laboratory system) for transitions to the isobaric analogs of the parent ground states. Column 8 gives the ratio of these cross sections to those calculated using spectroscopic amplitudes from the $f_{7/2}p_{3/2}$ model and with $W=3$.

The numbers in column 8 are normalizations (N) for $f_{7/2}p_{3/2}$ model calculations with the code TWOPAR. The fact that finite-range DWBA calculations performed[36-38] for the (t, p) reaction on both ^{40}Ca and ^{48}Ca resulted in equal values for N and also both the zero-range and finite-range calculations gave the same shapes for the angular distributions suggests that a normalization for TWOPAR is sensible and useful, at least for even-even targets. Bayman, from his study of the (t, p) reaction on ^{40}Ca and ^{48}Ca, obtained[39] an average N of 590 (for $W=1$). This value was obtained using spectroscopic amplitudes from the model of Bayman and Hintz.[40] Flynn and Hansen,[41] studying the (t, p) reaction on several targets from Ca to Pb, found an N of 310 (with $W=1$). The numbers given by Bayman, and by Flynn and Hansen are in fair agreement with our values, which range from 360 to 840 for $W=1$ (130 to 280 for $W=3$), obtained from $L_{np}=0$ $T=1$ transfers with the (^{3}He, p) reaction.

The last column in Table X gives the ratios of transitions to isobaric analog states calculated with the $f_{7/2}p_{3/2}$ model to that calculated with the $f_{7/2}$ model. This ratio increases from 2.6 to 4.4 with increasing A. The cross sections are greater in the $f_{7/2}p_{3/2}$ model than in the $f_{7/2}$ model because the DWBA transition amplitude favors the $2p_{3/2}$ level over all other levels in the sd or pf shells (see, for example, Table 2 of Ref. 36). With increasing A the transfer to the $p_{3/2}$ level becomes more important in the $f_{7/2}p_{3/2}$ model.

D. Comparison of calculations with experimental results: ^{45}Sc and ^{46}Ti targets

Since the $f_{7/2}p_{3/2}$ model for these nuclei is very complex, calculations were performed only with the $f_{7/2}$ model. Ratios of the summed $L_{np}=0+2$ cross sections to the cross sections for populating the analogs are given in Table XI. The experimentally determined ratio for the ^{45}Sc(^{3}He, p)^{47}Ti reaction is in good agreement with the calculations for $W=3$, whereas the ratios with the even-A Ca isotopes favors $W=1$. For the other odd-A target studied, ^{43}Ca, the uncertainty in the experimentally determined ratio precludes a choice for W.

In contrast to the case with the ^{45}Sc target, the model prediction for the ^{46}Ti target is in poor agreement with the experimentally determined ratio. Since the (^{3}He, p) reaction on the neighboring nuclei ^{45}Sc and ^{46}Ti yield about the same N (for the isobaric analog states) it might be supposed that the disagreement between theory and experiment is due to insufficient $L_{np}=0+2$ strength in the theory. This conclusion is not necessarily correct, though, for there is a factor of about 2 difference between N's obtained with the ^{43}Ca and ^{44}Ca targets, yet the theoretically determined ratios are in good agreement with the experimental ratios. Hence, we can only note that the summed $L_{np}=0+2$ strength relative to the analog strength is significantly less in the model than in the experiment for the (^{3}He, p) reaction on ^{46}Ti.

E. Systematics of $L_{np} = 0 + 2$ and 0 transitions

From Fig. 12 it is immediately evident that results with odd-A targets are distinctly different from those of even-even targets. This difference is not due to greater fragmentation with odd-A targets as, for example, more states are reached in ^{48}Sc by $L_{np} = 0 + 2$ than in ^{47}Ti. That the summed $L_{np} = 0 + 2$ strength, taken from Table V, is much smaller in odd-A nuclei than in even-even nuclei can be seen in Fig. 16(a). This result was unexpected since Hansen and Nathan,[1] from a study of the (^{3}He, p) reaction on even-even nuclei, found that the sums of the cross sections for $L_{np} = 0 + 2$ are approximately constant for f-shell nuclei. The $L_{np} = 0$ strength [Fig. 16(b)] scatters much less than the summed $L_{np} = 0 + 2$ strength and, in particular, there is no striking systematic difference between the results for even-even and odd-A targets.

The trend with mass number for the cross sections with $L_{np} = 0$ can be compared with the shell-model calculations. For the Ca targets with $A = 42$, 44, and 46, the $L_{np} = 0$ cross sections are observed to decrease with increasing A and calculations with both models reproduce this feature [see Fig. 17(b)]. The experimentally determined $L_{np} = 0$ strength for a ^{46}Ti target is more than two times that for a ^{46}Ca target and this fact is also reproduced by the $f_{7/2}$ model. (Calculations for a ^{46}Ti target were not carried out with the $f_{7/2}p_{3/2}$ model.) The $L_{np} = 0$ strength for the odd-A targets, relative to this strength for even-even targets, is also satisfactorily reproduced by the calculations.

Now we shall compare the systematics for the sum of the cross sections with $L_{np} = 0 + 2$ with the results of the shell-model calculations. The calculated relative cross section sums are shown in Fig. 17(a), the $f_{7/2}p_{3/2}$ and $f_{7/2}$ model results given by squares and triangles, respectively. One immediately sees that the calculations are in serious disagreement with the observed trend of the sum of the cross sections with mass number. Experimentally, the summed $L_{np} = 0 + 2$ strength for even-even targets, decreases in going from ^{42}Ca to ^{44}Ca and then increases in going to ^{46}Ca. The calculations indicate a monotonic decrease from ^{42}Ca to ^{46}Ca. The $f_{7/2}p_{3/2}$ model gives a sum for transitions to ^{45}Sc which is much larger than for transitions to even-A final nuclei. The $f_{7/2}$ model gives the same result; here the summed strength for both odd-A targets is higher than the summed strength for the neighboring even-even targets, in disagreement with experimental results. One might hope that the calculations would better reproduce the observed trend in the sum if the $2p_{1/2}$ and other shells were included. However, for several reasons we suspect that the discrepancy is due, not to a limited model space, but to some other effect. From Fig. 17(a) it is clear that the situation is no better with the $f_{7/2}p_{3/2}$ model than it is with the $f_{7/2}$ model. Secondly, it should be remembered that both models show the same trend with mass number in the ratio of the sum of the cross sections for $L_{np} = 0 + 2$ to the cross section for populating the isobaric analog state. In these two respects an extended model space did not help. That the finite-range calculations of Bayman[36] gave cross sections a factor of 3

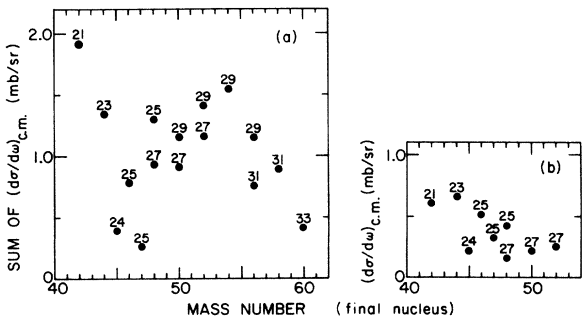

FIG. 16. (a) The sum of the differential cross sections for np transfers characterized by $L_{np} = 0 + 2$. (b) The differential cross sections for populating the isobaric analogs of the ground states of the parent nuclei. The numbers of neutrons in the final nuclei are given in the figures. (See Table V for a summary of the data).

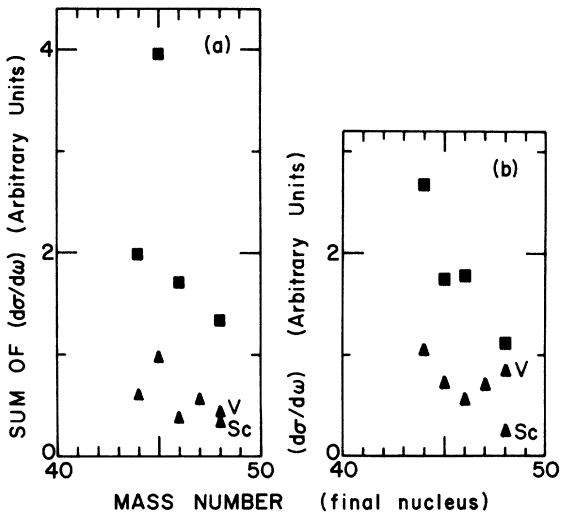

FIG. 17. (a) Calculated sums of the differential cross sections for $L_{np} = 0 + 2$. (b) Calculated differential cross sections for $L_{np} = 0$ (analogs of ground states). Calculations with the $f_{7/2}$ and $f_{7/2}p_{3/2}$ models are indicated by triangles and squares, respectively.

different than the experimental results strongly suggests that something is missing from the calculations.

IV. SUMMARY AND CONCLUSIONS

The sums of the cross sections for $L_{np} = 0 + 2$ vary considerably for $1f_{7/2}$ shell target nuclei. Of particular note is that for the odd-A targets, ^{43}Ca and ^{45}Sc. These sums are considerably lower than those for even-even target nuclei. Some of the strength could have been missed in the experiments; however, a factor of 2 error is unlikely.

Cross section calculations were made using both $f_{7/2}$ and $f_{7/2}p_{3/2}$ model spaces. The ratio of the summed $L_{np} = 0 + 2$ strength to the $L_{np} = 0$ strength is roughly comparable in the two models. Hence, while the dominant p-shell transfer is not directly included in the $f_{7/2}$ model, the missing strength must, in some sense, be similar for both the $L_{np} = 0 + 2$ and $L_{np} = 0$ transitions. In general, the agreement between the calculated and experimentally determined ratios is good except that the observed ratios are significantly greater for ^{46}Ca and ^{46}Ti targets.

The trend with mass number of the experimentally determined $L_{np} = 0$ cross sections is reproduced quite well by the calculations with both models. However, the agreement between the experimental results and calculations is unsatisfactory for the summed $L_{np} = 0 + 2$ strength. In particular, while the experimentally determined sums for odd-A targets are much lower than for neighboring even-even targets, the calculations give higher sums.

Comparing observed cross sections for $T = 1$ transfers with calculations using the zero-range DWBA code TWOPAR permitted a normalization of TWOPAR. Since the $f_{7/2}p_{3/2}$ model is not entirely successful, and since the values for the normalization vary by over a factor of 2 (see Table X), and since the concept of a single normalization for a range of nuclei has not been established, no single normalization factor can be extracted. However, the range of normalization values found here agree to within a factor of 2 with those obtained from a study of the (t, p) reaction on a wide range of targets.

Our comparison between the calculations and experimental data resulted in conflicting values for W. This must be considered as a shortcoming of the calculations.

Enlarging the model space from the $f_{7/2}$ shell to include all $f_{7/2}p_{3/2}$ configurations did not improve the agreement with the experimental results. This suggests that a further enlargement of the model space may not significantly improve the agreement. In addition an indication that the reaction mechanism is incompletely understood is that the finite-range calculations[37] for the (t, p) reaction on ^{40}Ca and ^{48}Ca targets predicted cross sections about a factor of 3 too low. It may be, for example, that two-step or higher processes are required and these corrections may affect even-even targets differently than odd-A targets.

ACKNOWLEDGMENTS

We are grateful to F. G. Karasek of the Materials Science Division of the Argonne National Laboratory for preparing the rolled targets. One of us (G.H.) wishes to thank the Western Michigan University Office of Research Services for partial support of this work through a faculty research grant.

---

*Work performed under the auspices of the U.S. Atomic Energy Commission.

[1]O. Hansen and O. Nathan, Phys. Lett. 39B, 419 (1972).
[2]J. W. Smith, L. Meyer-Schützmeister, G. Hardie, and P. P. Singh, Phys. Rev. C 8, 2232 (1973).
[3]J. W. Smith, L. Meyer-Schützmeister, T. H. Braid, P. P. Singh, and G. Hardie, Phys. Rev. C 7, 1099 (1973).
[4]T. Caldwell, O. Hansen, and D. J. Pullen, Nucl. Phys. A198, 529 (1972).
[5]J. R. Erskine, Argonne National Laboratory Report No. ANL-7641, 1969 (unpublished).
[6]J. R. Erskine, Argonne National Laboratory Report No. ANL-7728, 1970 (unpublished).
[7]J. R. Erskine and R. H. Vonderohe, Nucl. Instrum. Methods 81, 221 (1970).
[8]L. Meyer-Schützmeister, J. W. Smith, G. Hardie, H. Siefken, K. T. Knöpfle, M. Rogge, and C. Mayer-Böricke, Nucl. Phys. A199, 593 (1973).
[9]The calculations have been performed with the code TWOPAR. We are grateful to B. F. Bayman for having made this code available to us.
[10]A. H. Wapstra and N. B. Gove, Nucl. Data A9, 267 (1971).
[11]W. Schlegel, D. Schmitt, R. Santo, and F. Pühlhofer, Nucl. Phys. A153, 502 (1970).
[12]J. J. Schwartz and W. P. Alford, Phys. Rev. 149, 820 (1966).
[13]H. Ohnuma, Phys. Rev. C 3, 1192 (1971).
[14]R. R. Betts, H. T. Fortune, J. D. Garrett, R. Middleton, and D. J. Pullen, Phys. Rev. Lett. 26, 1121 (1971).
[15]L. Meyer-Schützmeister and D. S. Gemmell, Phys. Rev. Lett. 27, 869 (1971).
[16]Z. P. Sawa, J. Blomquist, and W. Gullholmer, Nucl. Phys. A205, 257 (1973).
[17]D. G. Fleming, R. A. Broglia, K. Abdo, O. Nathan, D. J. Pullen, B. Rosner, and O. Hansen, Phys. Rev.

C 5, 1356 (1972).
[18]N. J. A. Rust, W. J. Naudé, J. W. Koen, and W. L. Mouton, Nucl. Phys. A219, 232 (1974).
[19]R. J. Peterson and D. M. Perlman, Nucl. Phys. A117, 185 (1968).
[20]R. O. Ginaven and A. M. Bernstein, Nucl. Phys. A154, 417 (1970).
[21]F. Pühlhofer, Nucl. Phys. A116, 516 (1968).
[22]D. G. Fleming, O. Nathan, H. B. Jensen, and O. Hansen, Phys. Rev. C 5, 1365 (1972).
[23]O. Hansen and O. Nathan, Phys. Rev. Lett. 27, 1810 (1971).
[24]O. Hansen, J. J. Mulligan, and D. J. Pullen, Nucl. Phys. A167, 1 (1971).
[25]R. R. Betts, D. J. Pullen, and O. Hansen, Nucl. Phys. A182, 69 (1972).
[26]G. Hardie, T. H. Braid, L. Meyer-Schützmeister, and J. W. Smith, Phys. Rev. C 7, 2466 (1973).
[27]L. L. Lynn, R. C. Schaller, D. A. Barbour, T. A. Belote, and W. E. Dorenbusch, Nucl. Phys. A182, 272 (1972).
[28]M. Moinester, J. P. Schiffer, and W. P. Alford, Phys. Rev. 179, 984 (1969).
[29]J. B. McGrory and E. C. Halbert, Phys. Lett. 37B, 9 (1971).
[30]T. T. S. Kuo and G. E. Brown, Nucl. Phys. A114, 241 (1968).
[31]D. Gloeckner, to be published.
[32]I. S. Towner and J. C. Hardy, Advan. Phys. 18, 401 (1969).
[33]J. M. Nelson, N. S. Chant, and P. S. Fischer, Nucl. Phys. A156, 406 (1970).
[34]J. C. Hardy and I. S. Towner, Phys. Lett. 25B, 8 (1967).
[35]D. G. Fleming, J. Cerny, C. G. Maples, and N. K. Glendenning, Phys. Rev. 166, 1012 (1968).
[36]B. F. Bayman, Nucl. Phys. A168, 1 (1971).
[37]B. F. Bayman, Phys. Rev. Lett. 25, 1768 (1970).
[38]B. F. Bayman and D. H. Feng, Nucl. Phys. A205, 513 (1973).
[39]B. F. Bayman, private communication.
[40]B. F. Bayman and N. M. Hintz, Phys. Rev. 172, 1113 (1968).
[41]E. R. Flynn and O. Hansen, Phys. Lett. 31B, 135 (1970).